**Princeton Plasma Physics Laboratory**

**PPPL-** 5117

PPPL-5117

# Inferring Magnetospheric Heavy Ion Density using EMIC Waves

Eun-Hwa Kim, Jay R. Johnson,
Hyomin Kim, and Dong-Hun Lee

February 2015

PRINCETON PLASMA PHYSICS LABORATORY

**Prepared for the U.S. Department of Energy under Contract DE-AC02-09CH11466.**

# Inferring Magnetospheric Heavy Ion Density Using EMIC waves

Eun-Hwa Kim[1,2], Jay R. Johnson[1,2], Hyomin Kim[3] , and Dong-Hun Lee[4]

---

Corresponding author: E.-H. Kim, Princeton Center for Heliophysics, Princeton University, P.O. Box 0451, Princeton, NJ 08543-0451, USA (ehkim@pppl.gov)

[1] Princeton Center for Heliophysics, Princeton University, Princeton, New Jersey, USA

[2] Princeton Plasma Physics Laboratory, Princeton University, Princeton, New Jersey, USA

[3] Center for Space Science and Engineering Research, Bradley Department of Electrical and Computer Engineering, Virginia Tech, Virginia, USA.

[4] School of Space Research, Kyung Hee University, Yongin, Gyeonggi, Korea.

We present a method to infer heavy ion concentration ratios from electromagnetic ion cyclotron (EMIC) wave observations that result from ion-ion hybrid (IIH) resonance. A key feature of the IIH resonance is the concentration of wave energy in a field-aligned resonant mode that exhibits linear polarization. These mode-converted waves at the IIH resonance are localized at the location where the frequency of a compressional wave driver matches the IIH resonance condition, which depends sensitively on the heavy ion concentration. This dependence makes it possible to estimate the heavy ion concentration ratio. In this paper, we evaluate the absorption coefficients at the IIH resonance at Earth's geosynchronous orbit for variable concentrations of $He^+$ and wave frequencies using a dipole magnetic field model. We found that the resonance only occurs for a limited range of wave frequency such that the IIH resonance frequency is close to, but not exactly the same as the crossover frequency. Using the wave absorption and observed EMIC waves from the GOES-12 satellite, we demonstrate how this technique can be used to estimate that the $He^+$ concentration is around 4% near $L$=6.6.

## 1. Introduction

The presence of heavy ions can have a profound impact on the time response of the magnetosphere to internal and external forcing and can play a significant role in plasma entry and transport processes within the magnetosphere and ionosphere. Although satellites have directly detected heavy ion compositions and densities [e.g., *Chappell*, 1982; *Horwitz et al.*, 1984; *Farrugia et al.*, 1989; *Craven et al.*, 1997; *Bouhram et al.*, 2005], accurate measurement is difficult because of spacecraft charging effects and low flux of low velocity particles. Consequently, significant attention has been given to indirect methods that employ ULF wave observations, which are affected by the presence of heavy ions. Field-line resonance eigenfrequencies have been used to estimate magnetospheric plasma mass densities [e.g., *Denton et al.*, 2004; *Menk et al.*, 2004; *Takahashi et al.*, 2006; *Nose et al.*, 2011]. Comparison of electron density from plasma wave observations with mass density inferred from field-line resonance eigenfrequency measurements indicate that the mean mass is significantly larger than the proton mass meaning that significant amount of heavy ions may be present [*Denton et al.*, 2004; *Takahashi et al.*, 2006]. However, Alfvén resonant modes do not contain sufficient constraints to distinguish between relative concentrations of heavy ions. On the other hand, because ULF waves at higher frequency, such as electromagnetic ion cyclotron (EMIC) waves, are particularly sensitive to heavy ion concentrations they may be particularly useful to constrain heavy ion abundances through indirect measurement [e.g., *Fraser et al.*, 2005; *Sakaguchi et al.*, 2013; *Min et al.*, 2014].

EMIC waves are low frequency waves typically in the Pc 1-2 (0.2-5Hz) frequency range that are excited below the proton gyrofrequency and are commonly observed in the plasmasphere and magnetosphere. The polarization of these waves has been generally reported to be left-hand and these waves are generated by proton temperature anisotropy [e.g., *Cornwall*, 1965; *Kennel* and *Petschek*, 1966; *Williams* and *Lyons*, 1974a, 1974b; *Taylor* and *Lyons*, 1976; *Samson et al.*, 1991; *Kozyra et al.*, 1997; *Jordanova et al.*, 2001; *Thorne et al.*, 2006]. *Fraser et al.* [2005] suggested that the edge of the detected by left-handed EMIC wave frequency could be assumed to the cutoff frequency and thus the heavy ion density ratio can be estimated.

Right-hand or linear polarizations of EMIC waves have also been reported [e.g., *Fraser* and *McPherron*, 1982; *Anderson et al.*, 1992, 1996; *Min et al.*, 2012] and their origin is not fully understood. Although linear polarization can result from refraction [*Rauch and Roux*, 1982; *Horne* and *Thorne*, 1993], absorption at high latitudes [*Horne and Thorne,* 1997] likely limits such polarizations to higher latitudes. *Denton et al.* [1996] suggested that the linear polarization may result from superposition of two waves, but the mechanism requires multiple waves and appropriate differences in phase.

Alternatively, *Lee et al.* [2008] suggested that linearly polarized EMIC waves can be generated via mode conversion near the ion-ion hybrid (IIH) resonance location. When the frequency of incoming compressional waves matches the IIH resonance condition in an increasing (or decreasing) heavy ion concentration or inhomogeneous magnetic field strength, energy from incoming compressional waves concentrates at the IIH resonance location and mode converts to EMIC waves. Wave simulations using multi-fluid codes showed that the mode-converted EMIC waves at the IIH resonance are strongly guided by the ambient magnetic field ($\mathbf{B}_0$) and have linear polarization [*Kim et al.*, 2008, 2013, 2015a].

The IIH resonance condition is apparent in the wave dispersion relation of compressional waves in the ion cyclotron frequency range,

$$n_\perp^2 \cong \frac{(\varepsilon_R - n_\parallel^2)(\varepsilon_L - n_\parallel^2)}{(\varepsilon_S - n_\parallel^2)}, \quad (1)$$

where $n$ is the wave refractive index, subscriptions of $\perp$ and $\|$ represent the perpendicular and parallel to $\mathbf{B}_0$, respectively, and $\varepsilon_{R,L,S}$ is the tensor elements for two ions [*Johnson et al.*, 1995],

$$\varepsilon_R(\varepsilon_L) \cong \frac{c^2}{V_A^2}\frac{\omega_{c1}\omega_{c2}}{\omega_{cut}}\frac{\omega \pm \omega_{cut}}{(\omega \pm \omega_{c1})(\omega \pm \omega_{c2})} \qquad (2)$$

and

$$\varepsilon_S \cong \frac{c^2}{V_A^2}\frac{\omega_{c1}^2\omega_{c2}^2}{\omega_{bb}^2}\frac{\omega^2 - \omega_{bb}^2}{(\omega^2 - \omega_{c1}^2)(\omega^2 - \omega_{c2}^2)}, \qquad (3)$$

where $\omega = 2\pi f$ is an angular frequency, $V_A$ is the Alfvén velocity, $\omega_c$ is an ion gyrofrequency, $\omega_{cut}$ is the cutoff frequency for $\varepsilon_R(\varepsilon_L)=0$, and $\omega_{bb}$ is the Buchsbaum resonance frequency (or bi-ion frequency) for $\varepsilon_S(\omega_{bb})=0$ [*Buchsbaum*, 1960]. The dispersion relation in Eq. (1) exhibits a resonance ($n_\perp \rightarrow \infty$) where

$$n_\|^2 = \varepsilon_S. \qquad (4)$$

In between two ion gyrofrequencies, this resonance is referred as the IIH resonance and the frequency ($\omega_{ii}$) for $\varepsilon_S(\omega_{ii})=n^2_\|(\omega_{ii})$ called the IIH frequency is a function of ion concentration ratio ($\eta_{ion}=N_{ion}/N_e$), the ambient magnetic field strength ($B_0$), and field-aligned wave number ($k_\|$), where $N_{e(ion)}$ is an electron (ion) number density. For perpendicular propagation ($n_\| \rightarrow 0$), the resonance condition of Eq. (4) becomes $\varepsilon_S(\omega_{bb})=0$, which is the condition of Buchsbaum resonance. In the MHD regime of $\omega << \omega_{ci}$, the resonance condition in Eq. (4) is reduced to $\omega = k_\| V_A$.

Because the IIH waves are expected to globally oscillate along the magnetic field line at Mercury, which is similar to the field line resonance at Earth, *Kim et al.* [2008] assumed that a field-aligned wavelength ($\lambda_\| = 2\pi/k_\|$) of the IIH waves is similar to the magnetic field line length and showed that $\omega_{ii}$ becomes a function of $\eta_{ion}$ at a specific location. Thus they suggested that $\eta_{ion}$ can be estimated using the detected ULF wave frequency of the field-line resonance.

Later, *Kazakov* and *Fulop* [2013] calculated the value of $k_{\parallel}$ where the mode conversion at the IIH resonance is maximized in the dipole magnetic field and argued that the maximum absorption of compressional waves always occurs near the crossover frequency ($\omega_{\mathrm{cr}}$),

$$\omega_{cr}^2 = \eta_1 \omega_{c2}^2 + \eta_2 \omega_{c1}^2 . \tag{5}$$

Thus, similar to *Othmer et al.* [1999], they suggested that $\eta_{\mathrm{ion}}$ can be estimated using crossover frequency at the IIH resonance location in the arbitrary planetary magnetosphere.

However, *Kim et al.* [2011] previously showed that at Mercury the IIH resonance can be efficient over a wide range of frequency relative to the crossover frequency ($0.5\omega_{\mathrm{cr}} \le \omega_{\mathrm{ii}} \le 0.9\omega_{\mathrm{cr}}$), thus *Kim* and *Johnson* [2014] argued that the crossover frequency cannot be generally used to infer $\eta_{ion}$ in the arbitrary planetary magnetosphere. Moreover, *Kim et al.* [2015b] showed that a relatively large absorption occurs in a wide range of $\eta_{ion}$ even for a single frequency waves at a specific location at Mercury, thus they concluded that the $\eta_{ion}$ at Mercury cannot be simply inferred from the frequency of field-aligned IIH waves.

While number of study of ULF waves at Mercury in the context of the IIH resonance has been performed [e.g., *Othmer et al.*, 1999; *Glassmeier et al.*, 2003, 2004; *Klimushkin et al.*, 2006; *Kim et al.*, 2008, 2011, 2013, 2015a, b], the detailed characteristics of EMIC waves generated via mode-conversion at the IIH resonance in the Earth's magnetosphere have not been thoroughly investigated. Although the sharply peaked dependence of mode conversion on $\omega$ with observed $B_0$ makes it possible to estimate $\eta_{\mathrm{ion}}$ from the detected ULF waves that mode-converted at the IIH resonance location [e.g., *Kazakov* and *Fulop*, 2013; *Kim et al.*, 2015b], the relative efficiency of wave energy absorption at the resonance in a realistic magnetospheric profile has not been studied at Earth.

The aim of this paper is to determine the wave energy absorption at the IIH resonance in the Earth's magnetosphere and to predict whether such mode-converted IIH waves could be used as a diagnostic tool to estimate heavy ion density concentration ratio at Earth. To achieve these goals, we evaluate the absorption coefficient for variable concentrations of $He^+$ and azimuthal and field-aligned wavenumbers at Earth's geosynchronous orbit.

The paper is structured as follows: The numerical model and wave dispersion relations using realistic magnetospheric parameters are described in Section 2. Section 3 contains numerical results showing the dependence of absorption coefficient on $He^+$ concentration ratio and wave frequency. The method to infer heavy ion density from the detected EMIC waves is presented in Section 4. The last section contains a brief discussion and the conclusions.

## 2. Model Description

We calculate the efficiency of mode conversion of a radially propagating compressional wave at the IIH resonance using a simplified 1D slab cold plasma model that captures the essential features of the IIH resonance [*Kim et al.*, 2011]. The slab model is a local approximation where *x*, *y*, and *z* correspond to radial, azimuthal, and field-aligned coordinates. Wave propagation in the cold and fluid model can be described by Maxwell's equations combined with fluid equations for ions and electrons (ignoring electron inertial effects and background gradients related to diamagnetic drift and density compressions) [*Kim et al.*, 2011],

$$\frac{c}{\omega}\frac{\partial \mathbf{Y}}{\partial x} = \mathbf{MY}, \qquad (6)$$

where

$$\mathbf{Y} = \begin{pmatrix} E_y \\ \dfrac{c}{\omega}\dfrac{\partial E_y}{\partial x} - i n_y E_x \end{pmatrix}$$

and (7)

$$\mathbf{M} = \begin{pmatrix} \dfrac{n_y \varepsilon_d}{n_z^2 - \varepsilon_s} & 1 + \dfrac{n_y^2}{n_z^2 - \varepsilon_s} \\ \dfrac{(n_z^2 - \varepsilon_r)(n_z^2 - \varepsilon_l)}{n_z^2 - \varepsilon_s} & -\dfrac{n_y \varepsilon_d}{n_z^2 - \varepsilon_s} \end{pmatrix}, \tag{8}$$

where $n_y$ is the refractive index in the azimuthal direction and $\varepsilon_d = (\varepsilon_r + \varepsilon_l)/2$. Eqs. (6)-(8) have been solved with a finite difference approach with nonuniform mesh [e.g., *Johnson et al.*, 1995; *Johnson* and *Cheng*, 1999; *Kim et al.*, 2011]. Figure 1a shows the computational domain of $6.1 \leq L \leq 7.1$ and an illustration of transmission and reflection coefficients. Incoming waves are assumed to propagate from the outer magnetosphere at $L$=7.1 and have a resonance at $L$=6.6. The wave solution is decomposed into WKB solution to determine reflection, transmission, and absorption coefficients at the boundaries.

The resonance condition at $L$=6.6 can be written as a function of $\omega$ and $\eta_{\mathrm{He}}$ from Eq. (4),

$$n_\parallel^2(\omega, \eta_{He}) = \varepsilon_s\left(\omega, \eta_{He}, B_0(L=6.6), N_e(L=6.6)\right). \tag{9}$$

For calculation, we adopt a dipole magnetic field model at the equator,

$$B_0 = \frac{B_S}{L^3}, \tag{10}$$

where $B_S = 3.1\times10^{-5}$ T is the magnetic field strength on Earth's surface at the equator, and an empirical electron density model at the equator [*Sheeley et al.*, 2001], which is used in EMIC wave calculations [e.g., *Chen et al.*, 2009],

$$N_{\mathrm{e}} = 1390\left(\frac{3}{L}\right)^{4.83}, \tag{11}$$

and these profiles are plotted in Figure 1a.

To examine how the presence of heavy ion affects the dispersion and controls the distance between the cutoff of the incoming compressional wave and resonance, Figure 1b shows an example of $n_\perp$ across $L$ for $\omega$ = 3.2Hz and 3.45%<$\eta_{\mathrm{He}}$<4%. In this figure, it is apparent that $n_\perp \rightarrow \infty$ at $L$=6.6, except for $\eta_{\mathrm{He}}$ = 3.57%, where wave dispersion is reduced to $\varepsilon_S(\omega_{cr})=n^2_{\|}(\omega_{cr})$ from Eq. (1). For $n_y$=0, wave equations in Eqs. (6)-(8) show that there is no singularity and no mode conversion occurs.

For $\eta_{\mathrm{He}}$ = 3.86%, the compressional waves have two cutoffs ($n_\perp \rightarrow 0$) and one resonance ($n_\perp \rightarrow \infty$) in the calculation domain, which is called a cutoff-resonance-cutoff triplet, while for $\eta_{\mathrm{He}}$ = 4% waves have one cutoff and resonance, which is called a cutoff-resonance pair [*Stix*, 1992]. These two cutoffs are readily seen from the dispersion relation shown in Eq. (1) at $n^2_{\|}=\varepsilon_r(\varepsilon_l)$ and they occur on either side of the IIH resonance $n^2_{\|}=\varepsilon_s$ [*Karney et al.*, 1979]. When waves have a cutoff-resonance-cutoff triplet, absorption at the IIH resonance can occur both as the wave leaks through the resonance as well as when the wave reflects off the inner cutoff and propagates back into the resonance, and the wave absorption can be as large as 100% [e.g., *Kim et al.*, 2011], which is a characteristic of cutoff-resonance-cutoff conditions [*Karney et al.*, 1979; *Ram et al.*, 1996; *Lin et al.*, 2010].

## 3. Absorption Coefficient at the Ion-ion Hybrid Resonance

By adopting plasma conditions seen in Figure 1a, we calculate the absorption coefficient of the compressional waves as a function of $\eta_{\mathrm{He}}$ for $\omega$=3.2Hz as shown in Figure 2. Because the azimuthal wavenumber, $n_y$, is one of important factors that control absorption [*Kim et al.*, 2011], we also consider several azimuthal wavenumbers, such as

$$n_y(\omega,\eta_{He}) = mn_{\parallel}(\omega,\eta_{He}) = K_y\sqrt{\varepsilon_S(L=6.6)}\,, \qquad (12)$$

where $m$ is the azimuthal wavenumber normalized to the field-aligned wavenumber and we examine cases with $m$=0, 0.1, 0.2, and 0.3, respectively.

In Figure 2, the absorption coefficient oscillates as a function of $\eta_{\mathrm{He}}$ due to the interference effect between incoming and reflected compressional waves that occurs when the waves encounter a cutoff-resonance-cutoff triplet as shown in Figure 1b. For $m$=0, at $\omega=\omega_{ii(L=6.6)}=\omega_{cr(L=6.6)}$ (for $\eta_{\mathrm{He}}$=3.57%), no absorption occurs, which is consistent with previous calculations [*Klimushkin et al.*, 2006; *Kim et al.*, 2011]. When $m$ increases, the maximum value of absorption decreases from ~95% for $m$=0 and 0.1 to 27% for $m$=0.3 and the value of $\eta_{\mathrm{He}}$ where the maximum absorption occurs shifts from 3.84% for $m$=0 to 4.06% for $K_y$=0.3.

We focus on the range of $\eta_{\mathrm{He}}$ ($\Delta\eta_{\mathrm{He}}$) where strong absorption at the IIH resonance occurs and we found that $\Delta\eta_{\mathrm{He}}$ is very narrow and slightly decreases from $\Delta\eta_{\mathrm{He}}\sim$ 1.7% for $m$=0 to $\Delta\eta_{\mathrm{He}}\sim$1.2% for $m$=0.3. Therefore, Figure 2 suggests that linearly polarized EMIC waves for $\omega$=3.2Hz (thus the normalized frequency to the local gyrofrequency at the resonance location $\Omega=\omega/\omega_{ci}$=0.31) can be effectively mode-converted from the incoming compressional waves only when plasma contains 3.3-5% $He^+$ plasma. Conversely, if linearly polarized EMIC waves are observed with $\Omega$=0.31 at $L$=6.6, $\eta_{\mathrm{He}}$ can be inferred to as 3.3-5% by assuming electron-$H^+$-$He^+$ plasma.

In order to investigate the frequency range as well as $He^+$ density range that allows strong absorption at $L$=6.6, we calculate the absorption coefficient of the compressional waves as a function of the normalized wave frequency to the local gyrofrequency ($\Omega$) and $\eta_{\mathrm{He}}$ for $m$=0, where $\Delta\eta_{\mathrm{He}}$ is maximized. The frequency range in Figure 2 is restricted to range of frequency that provides efficient mode conversion, which is close to the crossover frequency. Figure 3 shows the calculated absorption and the shaded regions in this figure represent that no wave absorption has been calculated. The figure clearly shows that most absorption occurs near the crossover frequency ($\Omega_{cr}$) with narrow $\Delta\Omega$ and $\Delta\eta_{He}$ (the maximum $\Delta\Omega$ and $\Delta\eta_{He}$ are ~ 0.02 and 1.8%, respectively). Therefore, $\eta_{He}$ can be inferred from the observed $\Omega$ using the results of Figure 3. In the next section, we show how to infer the heavy ion concentration ratio using detected EMIC waves.

## 4. Inferring Heavy Ion Concentration Ratio

Figure 4 shows an example of EMIC waves detected by the GOES-12 near the solar minimum that exhibits dominant power in linear polarization. In this figure, EMIC wave activity in the $H^+$ band occurs from 04:00 to 04:50 UT with frequencies ranging from ~0.35 to 0.45 Hz, and the wave polarization ellipticity ($e$) in the plane perpendicular to the local magnetic fields indicates that the waves are largely linearly polarized. In our study, linear polarization is defined as having $|e| < 0.2$ [e.g., *Anderson et al.*, 1992]. Note that the GOES-12 was located at 75°W geographic longitude and 11° off the geomagnetic equator for this event.

In order to calculate heavy ion density ratio we select wave frequencies at 4:15, 4:20, 4:25, and 4:30 UT and the maximum and minimum frequencies at each time are (UT, $\Omega_{min}^{obs}$, $\Omega_{max}^{obs}$) ≈ (4:15, 0.29, 0.3), (4:20, 0.29, 0.34), (4:25, 0.27, 0.35), and (4:30, 0.28, 0.32), respectively. We plot the frequency ranges as a horizontal bars and the average values ($\overline{\Omega}_{obs}$) between $\Omega_{min}^{obs}$ and $\Omega_{max}^{obs}$ as circles in Figure 3. Using the average frequencies, the $\eta_{He}$ can be inferred to 3.3, 3.4, 4.2, and 3.6 ± 0.6%, respectively. Here, the minimum density ratio can be estimated by assuming that the average frequency is the crossover frequency ($\overline{\Omega}_{obs} \approx \Omega_{cr}$) and $\eta_{He}$ is about 2.7, 2.8, 3.6, and 3.0, respectively. Because both $\Delta\Omega$ and $\Delta\eta_{He}$ are narrow, the estimated density ratio difference between maximum and minimum is approximately 1%, therefore the heavy ion density ratio can be estimated to reasonable accuracy by assuming the detected wave frequency is the crossover frequency, which is consistent with *Kazakov* and *Fulop* [2013], as well as by using Figure 3.

## 5. Discussion and Conclusion

In this paper, we present a method to infer a magnetospheric heavy ion concentration ratio using observed EMIC waves, which is mode-converted from compressional waves [*Lee et al.*, 2008]. At geosynchronous orbit near $L$=6.6, we show that compressional wave absorption at the IIH resonance (i.e., the linearly polarized EMIC wave generation) occurs over a limited range of wave frequencies near the crossover frequency. Therefore, $\eta_{\mathrm{He}}$ can be inferred from the observed EMIC waves at $L$=6.6. Interestingly, this result was predicted by *Kazakov* and *Fulop* [2013], although their approach does not provide an accurate estimate of wave absorption [*Kim and Johnson*, 2014]. Using the wave absorption and observed EMIC waves from the GOES-12 satellite, we also demonstrate how this technique can be used to estimate that the $He^+$ concentration is around 4% near $L$=6.6. Similarly, *Fraser et al.* [2005] estimated $\eta_{\mathrm{He}}$ to range between 6-16% at $L$=6.6 inferred from the GOES-8 and 10 observations of left-handed polarized EMIC waves.

Because the electron density affects the compressional wave dispersion relation, wave absorption at the IIH resonance can be modified by the radial structure of the electron density. Although we adopt an empirical density model [*Sheeley et al.*, 2001], the results showing that the maximum absorption of compressional waves occurs near the crossover frequency are consistent with *Kazakov* and *Fulop* [2013], which assumed a homogeneous electron density. However, in order to accurately estimate $\eta_{\mathrm{He}}$ using linear polarization EMIC waves, it is necessary to quantify $\Delta\eta_{\mathrm{He}}$ where strong absorption occurs. Thus we adopt three electron density models to calculate the wave absorption, including an empirical density model ($N_e^{empirical}$) [*Sheeley et al.*, 2001], a simple density model used in MHD simulations ($N_e^{simple}$) [*Lee and Lysak*, 1989], $N_e^{simple}=(10/L)^3$, and a homogeneous density of 33 cm$^{-3}$ ($N_e^{constant}$), which is the average value between $N_e^{empirical}$ and $N_e^{simple}$ at $L$=6.6.

Figure 5a shows the electron density profiles that have been used. The density gradient of the empirical model ($\nabla N_e^{empirical}$) is the largest of all the models. We calculate the absorption coefficient as a function of $\eta_{\mathrm{He}}$ at $L$=6.6 as shown in Figure 5b. Here, the strong absorption occurs for almost same ranges of $\Delta\eta_{\mathrm{He}}$ ($2.5\%<\eta_{\mathrm{He}}<5\%$), but $\Delta\eta_{\mathrm{He}}$ decreases when $\nabla N$ increases. This result suggests that $\Delta\eta_{\mathrm{He}}$ where strong absorption occurs is not sensitive to the radial structure of electron density profile. Therefore, we confirm our conclusion that $\eta_{\mathrm{He}}$ can be inferred from the observed EMIC waves at geosynchronous orbit using Figure 3, which is robust for typical magnetospheric parameters.

The method suggested in this paper can also be applied to other L-shells to estimate the global structure of magnetospheric heavy ion concentrations using observations of linearly polarized EMIC waves to infer density from the equivalent of Figure 3 constructed at each L-shell. Because the wave absorption is very sensitive to plasma conditions such as density scale length, heavy ion density ratio, and magnetic field gradient, it is expected that frequency ranges where strong absorption occurs might vary depending on different L-shells. For example at Mercury, the value of the frequency ratio to the crossover frequency with maximum absorption is $0.5\leq\omega_{ii}/\omega_{cr}\leq0.9$ [*Kim et al.*, 2011, 2015b; *Kim* and *Johnson*, 2014], which is much wider than $\omega_{ii}/\omega_{cr}\sim0.9$ at Earth's geosynchronous orbit.

For simplicity of presentation, in this paper we have ignored the effects of $O^+$. However, the $O^+$ concentration can be large at solar maximum [*Denton et al.*, 2011] and may even exceed the $H^+$ concentration throughout the nightside and around dawn [*Lee and Angelopoulos*, 2014]. In addition, EMIC waves are often observed in each pair of ion gyrofrequencies, such as $He^+$ band ($\omega_{co}<\omega<\omega_{cHe}$), and $O^+$ band ($\omega<\omega_{cO}$), and the IIH resonance also occurs between each pair of ion gyrofrequencies [e.g., *Kim et al.*, 2013]. It is straightforward to include the effects of $O^+$ in our model, and the inclusion of heavier ions would likely modify the frequency window for wave absorption. To constrain both $He^+$ and $O^+$ would require measurement of two bands corresponding to the two ion-ion hybrid resonances or utilization of another complementary method that constrains the total mass density using lower frequency waves [e.g., *Denton et al.*, 2011]. However, in order to confirm, further research in multi-heavy ion plasmas should be followed.

In summary, we present a method to infer heavy ion concentrations using detected EMIC waves from satellites at geosynchronous orbit. Because linearly polarized EMIC waves can be generated via mode conversion from compressional waves, peaked dependence of compressional wave absorption (thus generation of linearly polarized EMIC waves) enables us to estimate heavy ion concentration ratios. We demonstrated that the maximum absorption occurs when the IIH resonance frequency is close to the crossover frequency at geosynchronous orbit and inferred heavy ion densities around ~ 4% using an EMIC wave event observed by the GOES-12 data near solar minimum, which is consistent with previous estimations.

**Acknowledgements**. The authors thank to Prof. Mark Engebretson for his valuable comments. The work at the Princeton University was supported by NASA grants (NNH09AM53I, NNH09AK63I, and NNH11AQ46I), NSF grant ATM0902730, and DOE contract DE-AC02-09CH11466. The work at Virginia Tech was supported by NSF grant PLR-1243398. The work at the Kyung Hee University was also supported by the BK21 Plus Program through the National Research Foundation of Korea, funded by the Ministry of Education, Science and Technology. The GOES spacecraft data were provided by the NOAA Space Weather Prediction Center.

**References**

Anderson, B. J., R. E. Erlandson and L. J. Zanetti (1992), A statistical study of Pc 1-2 magnetic pulsations in the equatorial magnetosphere 1. Equatorial occurrence distributions, *J. Geophys. Res. 97*, 3075-3088.

Anderson, B. J., R. E. Denton and S. A. Fuselier (1996), On determining polarization characteristics of ion cyclotron wave magnetic field fluctuations, *J. Geophys. Res. 101*, 13195-13214.

Bouhram, M., B. Klecker, G. Paschmann, S. Haaland, H. Hasegawa, A. Blagau, H. R, J.-A. Sauvaud, L. M. Kistler and A. Balogh (2005), Survey of energetic $O^+$ ions near the dayside mid-latitude magnetopause with Cluster, *Ann. Geophys. 23*, 1281-1294.

Buchsbaum, S. J. (1960), Ion Resonance in a Multicomponent Plasma, *Phys. Rev. Lett 5*, 495-497.

Chappell, C. R. (1982), Initial observations of thermal plasma composition and energetics from Dynamics Explorer-1, *Geophys. Res. Lett. 9*, 929-932.

Chen, L., R. M. Thorne and R. B. Horne (2009), Simulation of EMIC wave excitation in a model magnetosphere including structured high-density plumes, *J. Geophys. Res. 114*, A07221, doi:10.1029/2009JA014204.

Cornwall, J. M. (1965), Cyclotron instabilities and electromagnetic emission in the ultra low frequency and very low frequency ranges, *J. Geophys. Res. 70*, 61, doi:10.1029/JZ070i001p00061.

Craven, P. D., D. L. Gallagher and R. H. Comfort (1997), Relative concentration of $He^+$ in the inner magnetosphere as observed by the DE 1 retarding ion mass spectrometer, *J. Geophys. Res. 102*, 2279-2290.

Denton, R. E., B. J. Anderson, G. Ho and D. C. Hamilton (1996), Effects of wave superposition on the polarization of electromagnetic ion cyclotron waves, *J. Geophys. Res. 101*, 24869-24886.

Denton, R. E., J. D. Menietti, J. Goldstein, S. L. Young and R. R. Anderson (2004), Electron density in the magnetosphere, *J. Geophys. Res. 109*, 09215.

Denton, R. E., M. F. Thomsen, K. Takahashi, R. R. Anderson and H. J. Singer (2011), Solar cycle dependence of bulk ion composition at geosynchronous orbit, *J. Goephys. Res. 116*, 3212.

Farrugia, C. J., J. Geiss, H. Balsiger and D. T. Young (1989), The composition, temperature, and density structure of cold ions in the quiet terrestrial plasmasphere - GEOS 1 results, *J. Geophys. Res. 94*, 11865-11891.

Fraser, B. J. and R. L. McPherron (1982), Pc 1-2 magnetic pulsation spectra and heavy ion effects at synchronous orbit - ATS 6 results, *J. Geophys. Res. 87*, 4560-4566.

Fraser, B. J., H. J. Singer, M. L. Andrian, D. L. Gallagher and M. F. Thomsen, (2005) The Relationship between Plasma Density Structure and Emic Waves at Geosynchronous Orbit., in *Inner Magnetosphere Interactions: New Perspectives from Imaging* (edited by J. L. Burch, M. Schulz, and H. Spence), American Geophysical Union, Washington, D. C., p55, doi: 10.1029/159GM04.

Glassmeier, K.-H., P. N. Mager and D. Y. Klimushkin (2003), Concerning ULF pulsations in Mercury's magnetosphere, *Geophys. Res. Lett. 30*, 1928.

Glassmeier, K.-H., D. Klimushkin, C. Othmer and P. Mager (2004), ULF waves at Mercury: Earth, the giants, and their little brother compared, *Adv. Space Res. 33*, 1875-1883, doi:10.1016/j.asr.2003.04.047.

Horne, R. B. and R. M. Thorne (1993), On the preferred source location for the convective amplification of ion cyclotron waves, *J. Geophy. Res. 98*, 9233, doi:10.1029/92JA02972.

Horne, R. B. and R. M. Thorne (1997), Wave heating of He+ by electromagnetic ion cyclotron waves in the magnetosphere: Heating near the $H^+$ - $He^+$ bi-ion resonance frequency, *J. Geophys. Res. 102*, 11457.

Horwitz, J. L., R. H. Comfort and C. R. Chappell (1984), Thermal ion composition measurements of the formation of the new outer plasmasphere and double plasmapause during storm recovery phase, *Geophys. Res. Lett. 11*, 701-704.

Johnson, J. R., T. Chang and G. B. Crew (1995), A study of mode conversion in an oxygen-hydrogen plasma, *Phys. Plasmas 2*, 1274-1284.

Johnson, J. R. and C. Z. Cheng (1999), Can ion cyclotron waves propagate to the ground?, *Geophys. Res. Lett. 26*, 671-674.

Jordanova, C. V. K., J. Farrugia, R. M. Thorne, G. V. Khazanov, G. D. Reeves and M. F. Thomsen (2001), Modeling ring current proton precipitation by electromagnetic ion cyclotron waves during the May 14-16, 1997, storm, *J. Geophys. Res. 106*, 7, doi: 10.1029/2000JA002008.

Karney, C. F. F., F. W. Perkins and Sun Y. C. (1979), Alfven resonance Effects on Magnetosonic Modes in Large Tokamaks, *Phys. Rev. Lett. 24*, 1621.

Kazakov, Y. O. and T. Fulop (2013), Mode Conversion of Waves in the Ion-Cyclotron Frequency Range in Magnetospheric Plasmas, *Phys. Rev. Lett. 111*, 125002.

Kennel, C. F. and H. E. Petschek (1966), Limit on stably trapped particle fluxes, *J. Geophys. Res. 71*, 1.

Kim, E. H., J. R. Johnson and D. H. Lee (2008), Resonant absorption of ULF waves at Mercury's magnetosphere, *J. Geophys. Res. 113*, A11207.

Kim, E.-H., J. R. Johnson and K.-D. Lee (2011), ULF wave absorption at Mercury, *Geophys. Res. Lett. 38*, L16111, doi:10.1029/2011GL048621.

Kim, E.-H., J. R. Johnson, D.-H. Lee and Y. S. Pyo (2013), Field-line resonance structure in Mercury's multi-ion magnetosphere, *Earth, Planets, and Space 65*, 447.

Kim, E.-H. and J. R. Johnson (2014), Comment on Mode Conversion of Waves in the Ion-Cyclotron Frequency Range in Magnetospheric Plasmas, *Phys. Rev. Lett. 113*, 089501.

Kim, E.-H., J. R. Johnson, E. Valeo and C. K. Phillips (2015a), Global modeling of ULF waves at Mercury, *Geophys. Res. Lett.*, submitted.

Kim, E.-H., S. A. Boardsen, J. R. Johnson and J. A. Slavin (2015b), ULF waves at Mercury, in *Low-Frequency Waves in Space Plasmas* (eds A. Keiling, D.-H. Lee, K.-H. Glassmeier, and M. N. Valery), American Geophysical Union, Washington, D. C., submitted.

Klimushkin, D. Y., P. N. Mager and K.-H. Glassmeier (2006), Axisymmetric Alfven resonances in a multi-component plasma at finite ion gyrofrequency, *Ann. Geophys. 24*, 1077-1084.

Kozyra, J. U., V. K. Jordanova, R. B. Home and R. M. Thorne, (1997) Modeling of the contribution of electromagnetic ion cyclotron (EMIC) waves to stormtime ring current erosion., in *Magnetic Storms* (edited by Tsurutani, B. T., W. D. Gonzalez, Y. Kamide and J. K. Arballo), AGU., Washington, D. C., 187, doi: 10.1029/GM098.

Lee, J. H. and V. Angelopoulos (2014), On the presence and properties of cold ions near Earth's equatorial magnetosphere, *J. Geophy. Res. 119*, 1749–1770.

Lee, D.-H., J. R. Johnson, K. Kim and K.-S. Kim (2008), Effects of heavy ions on ULF wave resonances near the equatorial region, *J. Geophys. Res. 113*, A11212, doi:10.1029/2008JA 013088.

Lee, D.-H. and R. L. Lysak (1989), Magnetospheric ULF wave coupling in the dipole model - The impulsive excitation, *J. Geophys. Res. 94*, 17097-17103.

Lin, Y., J. R. Johnson and X. Y. Wang (2010), Hybrid simulation of mode conversion at the magnetopause, *J. Geophys. Res. 115*, A04208.

Menk, F. W., I. R. Mann, A. J. Smith, C. L. Waters, M. A. Clilverd and D. K. Milling (2004), Monitoring the plasmapause using geomagnetic field line resonances, *J. Geophys. Res. 109*, 4216.

Min, K., J. Lee, K. Keika and W. Li (2012), Global distribution of EMIC waves derived from THEMIS observations, *J. Geophys. Res. 117*, A05219, doi:10.1029/2012JA017515.

Min, K., K. Liu, J. W. Bonnell, A. W. Breneman, R. E. Denton, H. O. Funsten, J.-M. Jahn, C. A. Kletzing, W. S. Kurth, B. A. Larsen, G. D. Reeves, H. E. Spence and J. R. Wygnant (2014), Study of EMIC Wave Excitation Using Direct Ion Measurements, *J. Geophys. Res.*, submitted.

Nose, M., K. Takahashi, R. R. Anderson and H. J. Singer (2011), Oxygen torus in the deep inner magnetosphere and its contribution to recurrent process of O+-rich ring current formation, *J. Geophys. Res. 116*, 10224.

Othmer, C., K.-H. Glassmeier and R. Cramm (1999), Concerning field line resonances in Mercury's magnetosphere, *J. Geophys. Res. 104*, 10369-10378.

Ram, A. K., A. Bers and S. D. Schultz (1996), Mode conversion of fast Alfv\'en waves at the ion-ion hybrid resonance, *Phys. Plasmas 3*, 1828.

Rauch, J. L. and A. Roux (1982), Ray tracing of ULF waves in a multicomponent magnetospheric plasma - Consequences for the generation mechanism of ion cyclotron waves, *J. Geophys. Res. 87*, 8191-8198.

Sakaguchi, K., Y. Kasahara, M. Shoji, Y. Omura, Y. Miyoshi, T. Nagatsuma, A. Kumamoto and A. Matsuoka (2013), Akebono observations of EMIC waves in the slot region of the radiation belts, *Geophy. Res. Lett. 40*, 5587-5591.

Samson, J. C., T. J. Hughes, F. Creutzberg, D. D. Wallis, R. A. Greenwald and J. M. Ruohoniemi (1991), Observations of a detached, discrete arc in association with field line resonances, *J. Geophys. Res. 96*, 15683, doi:10.1029/91JA00796.

Sheeley, B. W., M. B. Moldwin, H. K. Rassoul and R. R. Anderson (2001), An empirical plasmasphere and trough density model: CRRES observations, *J. Geophys. Res. 106*, 25631.

Stix, T. H. (1992), *Waves in plasmas*. New York,: American Institute of Physics.

Takahashi, K., R. E. Denton, R. R. Anderson and W. J. Hughes (2006), Mass density inferred from toroidal wave frequencies and its comparison to electron density, *J. Geophys. Res. 111*, 1201.

Taylor, W. W. L. and L. R. Lyons (1976), Simultaneous equatorial observations of 1- to 30-Hz waves and pitch angle distributions of ring current ions, *J. Geophys. Res. 81*, 6177, doi:10.1029/JA081i034p06177.

Thorne, R. M., R. B. Horne, V. K Jordanova, J. Bortnik and S. Glauert, (2006) Interaction of EMIC Waves With Thermal Plasma and Radiation Belt Particles., in *Magnetospheric ULF Waves: Synthesis and New Directions* (edited by Takahashi, K., P. J. Chi, R. E. Denton and R. L Lysak), AGU, Washington, D. C., 213, doi: 10.1029/169GM14.

Williams, D. J. and L. R. Lyons (1974a), Further aspects of the proton ring current interaction with the plasmapause: Main and recovery phases, *J. Geophys. Res. 79*, 4791, doi:10.1029/JA079i031p04791.

Williams, D. J. and L. R. Lyons (1974b), The proton ring current and its interaction with the plasmapause: Storm recovery phase, *J. Geophy. Res. 79*, 4195, doi:10.1029/JA079i028p04195.

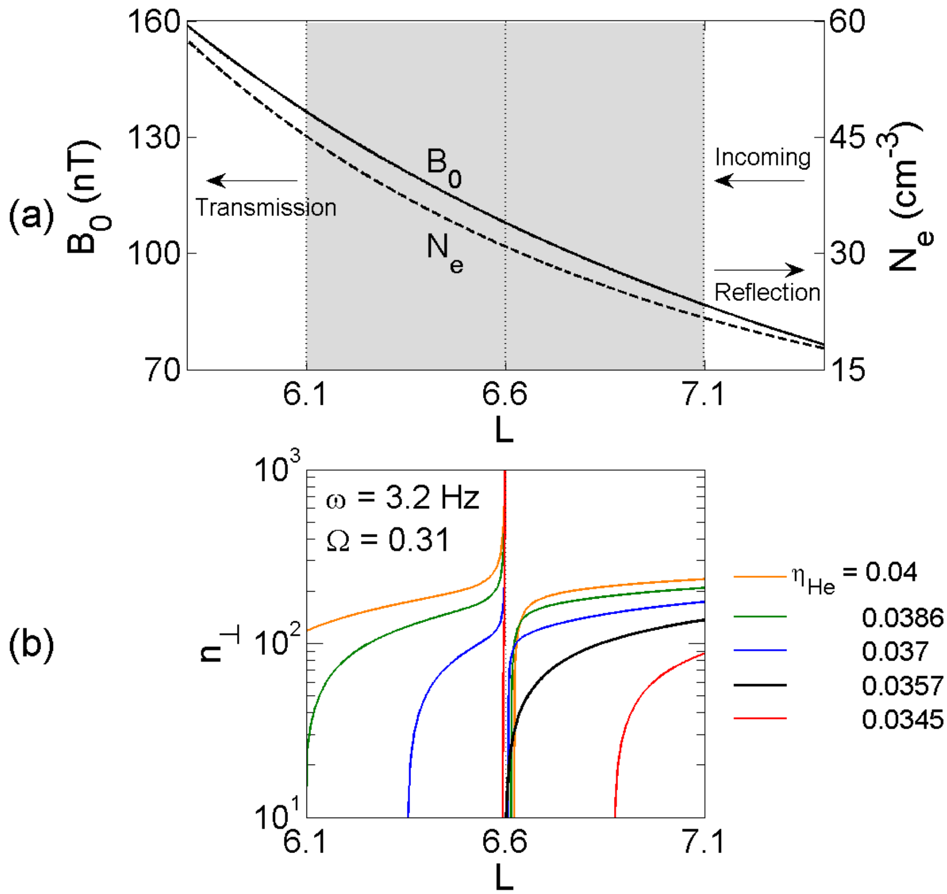


Figure 1. (a) The ambient magnetic field ($B_0$, solid line) and electron density ($N_e$, dashed line) in the radial direction. Dotted vertical lines are the resonance location at $L$=6.6 and spatial calculation boundaries at $L$=6.1 and 7.1. (b) The refractive index $n_\perp$ of incoming compressional waves of $\omega$=3.2Hz ($\Omega=\omega/\omega_{ci(L=6.6)}$=0.31) for $\eta_{He} = N_{He}/N_e$ = 4% (orange), 3.86% (green), 3.7% (blue), 3.57% (black) and 3.45% (red), respectively. In this case, the IIH resonance is assumed to occur at $L$=6.6.

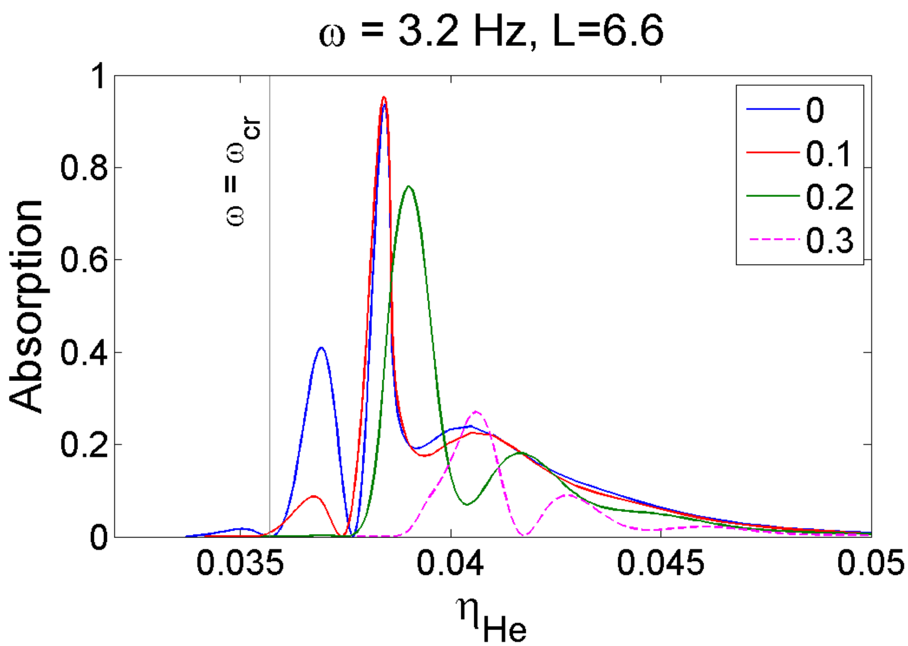


Figure 2. The absorption coefficient for $\omega = 3.2$ Hz as a function of $\eta_{He}$ at $L$=6.6 for $m$=0 (blue), 0.1 (red), 0.2 (green) and 0.3 (magenta), respectively, where $m$ is the azimuthal wavenumber normalized to the field-aligned wavenumber.

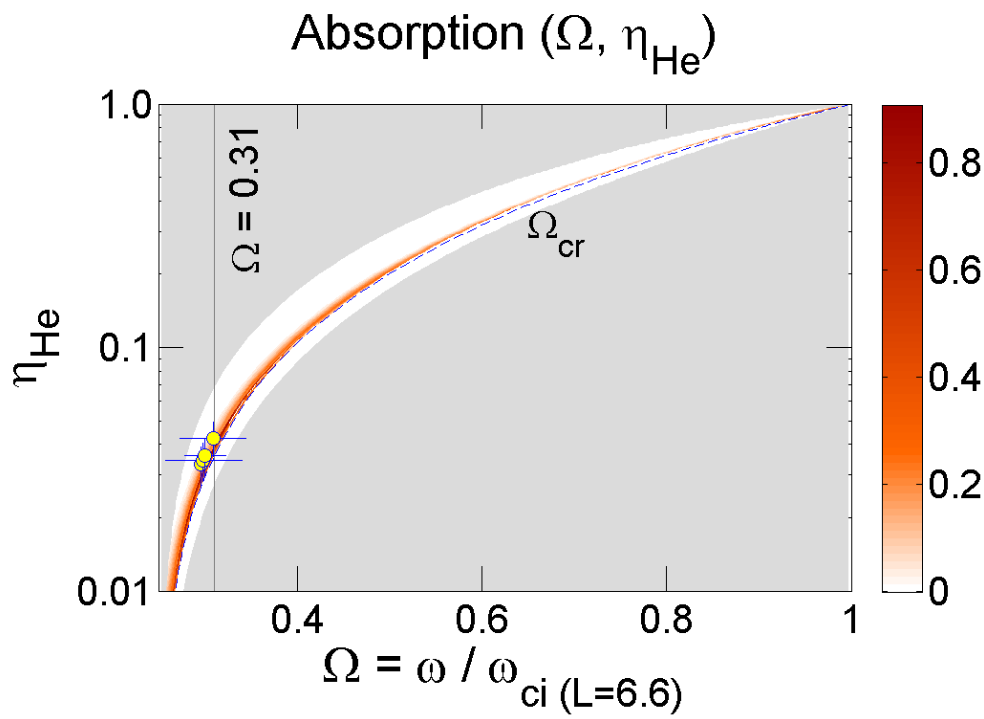


Figure 3. The absorption coefficient as a function of $\Omega$ and $\eta_{He}$. The shaded regions in this figure represent that no wave absorption has been calculated. The circles signify individual averaged wave frequencies detected by GOES-12 on 4:15, 4:20, 4:25, and 4:30UT from Figure 4. The crosses are the maximum and minimum frequency detected by the GOES satellite ($\overline{\Omega}_{obs}$) and helium concentration ratio ranges calculated in this letter. Using the average frequencies, $\eta_{He}$ can be inferred to 3.3, 3.4, 4.2, and 3.6 ± 0.7%, respectively. Here, the minimum density ratio can be estimated by assuming that the average frequency is the crossover frequency ($\overline{\Omega}_{obs} \approx \Omega_{cr}$).

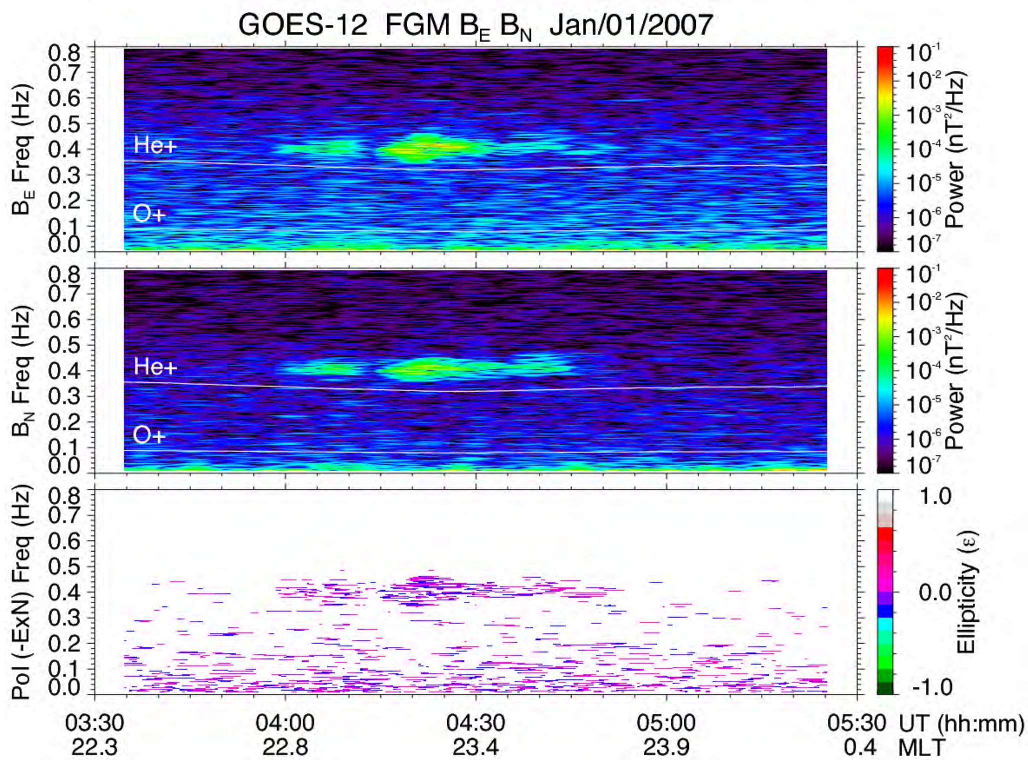


Figure 4. High-time resolution (512ms) Level 2 GOES-12 magnetic field data showing EMIC wave activity in the $H^+$ band from 04:00 to 04:50 UT over the frequencies of ~0.35 to 0.45 Hz. The top and middle panels present wave power as a function of frequency in the E and N components of the data, respectively. The GOES satellite magnetometers conform to the PEN coordinate system, in which $B_P$ is a magnetic field vector component pointing northward, perpendicular to the orbit plane (parallel to Earth's spin axis) and $B_E$ points earthward, being perpendicular to $B_P$, $B_N$ completes the Cartesian coordinates and points eastward. Wave polarization ellipticity in the plane perpendicular to the local magnetic fields (E and N) is shown in the bottom panel, indicating that the wave is largely linearly polarized. Note that only linear power ($|e|<0.2$) is displayed.

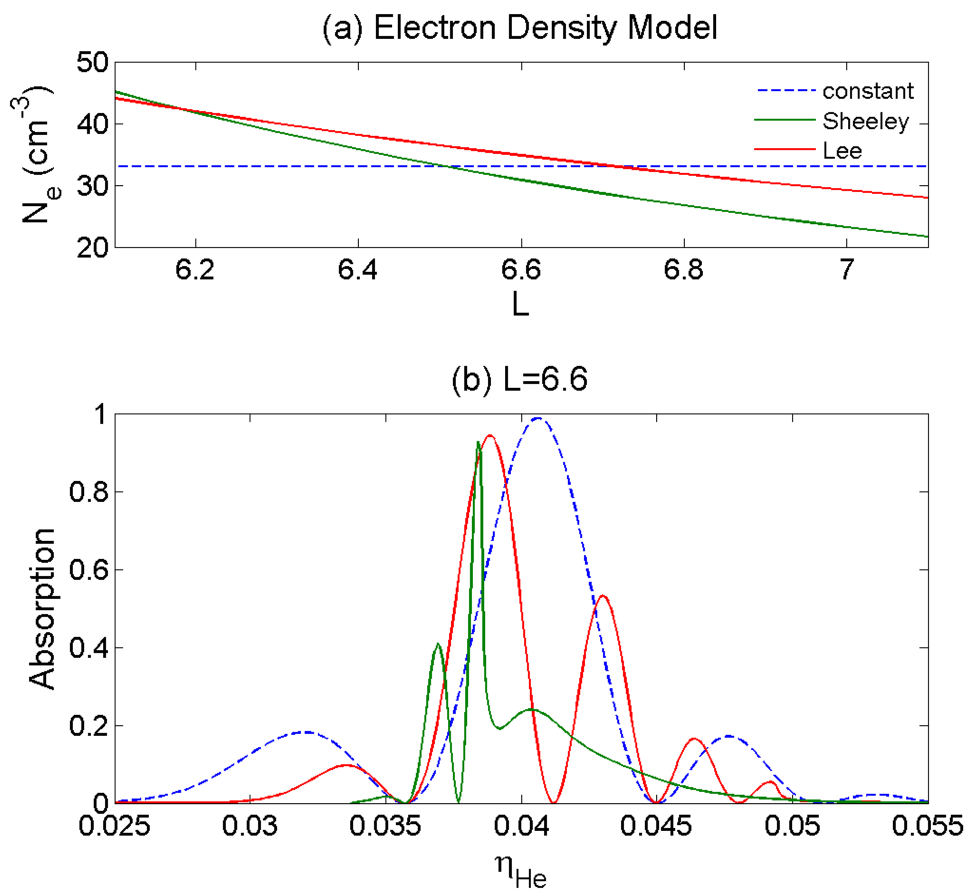


Figure 5. (a) The adopted magnetospheric electron density model: a simple density model used by MHD wave simulations of *Lee and Lysak* [1989] (red solid line), an empirical density model by *Sheeley et al.* [2001] (green solid line), and a homogeneous density of $N_e$ = 33 cm$^{-3}$ (blue dashed line); (b) absorption coefficient of compressional waves as a function of $L$ for $\omega$=3.2Hz and $\eta_{\mathrm{He}}$=3.84% by adopting three electron density models shown in Figure 5(a).

Princeton Plasma Physics Laboratory
Office of Reports and Publications

Managed by
Princeton University

under contract with the
U.S. Department of Energy
(DE-AC02-09CH11466)

P.O. Box 451, Princeton, NJ 08543
Phone: 609-243-2245
Fax: 609-243-2751
E-mail: publications@pppl.gov
Website: http://www.pppl.gov